

Experimental Study on Transmission of an Overdriven Detonation Wave Across a Mixture

J. Li¹, K. Chung², W.H. Lai¹, and F.K. Lu³

¹ *National Cheng Kung University, Institute of Aeronautics and Astronautics, Tainan, Taiwan*

² *National Cheng Kung University, Aerospace Science and Technology Research Center, Tainan, Taiwan*

³ *University of Texas at Arlington, Mechanical and Aerospace Engineering Department, Aerodynamics Research Center, Arlington, Texas, USA*

Summary. Two sets of experiments were performed to achieve a strong overdriven state in a weaker mixture by propagating an overdriven detonation wave via a deflagration-to-detonation transition (DDT) process. First, preliminary experiments with a propane/oxygen mixture were used to evaluate the attenuation of the overdriven detonation wave in the DDT process. Next, experiments were performed wherein a propane/oxygen mixture was separated from a propane/air mixture by a thin diaphragm to observe the transmission of an overdriven detonation wave. A simple wave intersection model showed that the rarefaction effect must be included to ensure that the post-transmission wave properties are not overestimated. The experimental results showed that the strength of the incident overdriven detonation plays an important role in the wave transmission process. After the wave transmission process, the propagation of the detonation directly correlates with detonability limits.

1 Introduction

The phenomenon of the transmission of detonation from one mixture to another of different sensitivity is of interest in the development of pulse detonation engines (PDEs). To ensure the success of a PDE, a predetonator concept has been proposed [1]. A detonation wave can then be generated with relative ease in the predetonator filled with an energetic material and transmitted into a larger diameter, main combustor filled with a gaseous or liquid hydrocarbon-air mixture. Nevertheless, Schultz and Shepherd [2] indicated that a detonation wave with a $C_3H_8 + 5O_2$ mixture failed to transmit into a larger tube with a $C_3H_8 + 5(O_2 + \beta N_2)$ mixture ($\beta \geq 0.76$). On the other hand, Desbordes and Lannoy [3] showed that a Chapman-Jouguet (CJ) detonation wave propagating into a less sensitive mixture can result in an overdriven detonation condition, in which the cell width decreases with a higher degree of overdrive D^* and in turn a decrease in the diffraction critical diameter. Here the diffraction critical diameter is the minimum tube diameter for the successful transmission of a detonation wave through an abrupt area expansion. This result can be applied in the predetonator concept to let the detonation wave propagate across a mixture change prior to an area change. Furthermore, in some cases, an overdriven detonation wave was observed in the deflagration-to-detonation transition (DDT) process [4]. It can therefore be expected that an overdriven detonation wave propagating into a less sensitive mixture may sustain a detonation wave with some degree of overdrive than the propagation of a CJ detonation wave. Transmission of detonation waves across a mixture change has been studied from the 1950s. These studies, however, did not examine the transmission of an overdriven detonation wave in detail. For such reasons, the present work examines the transmission of an overdriven detonation from a C_3H_8/O_2 mixture to a C_3H_8/air mixture.

2 Experimental Setup

A preliminary test concerning the relation between the degree of overdrive and the length of the detonation wave decay was carried out. Four smooth, aluminum 6061-T6 tubes, 914.4 mm long with inner tube diameters $d = 25.4, 50.8, 101.6,$ and 152.4 mm were used. It must be noted that the tube diameter used in the next set of experiments was $d = 50.8$ mm because this size is near the detonability limits of a stoichiometric C_3H_8/air mixture. Here the detonability limit is the propagation limit of a stable, self-sustained detonation. For the smooth-wall tube, detonability limit is $d \geq \lambda_{CJ}$ [5].

A weak ignition system was used at the closed end. After evacuating the tube to 20–30 Pa, propane and O_2 were pumped into the tube. To ensure the homogeneity of the mixture, a circulation pump was used. In addition, the concentration of the mixture was calibrated by gas chromatography (CHINA 9800 GC/TCD) for each run. The uncertainty of the equivalence ratio was ± 0.05 for 95% confidence. Signals from the sensors were digitized and stored in LeCroy 6810 high-speed data acquisition modules, typically at 500 ksamples/s. Five piezoelectric pressure transducers (PCB 112A) were mounted along the streamwise direction to estimate the propagation speed of the detonation wave. A nonstationary cross-correlation technique (NCCF) [6] was adopted to compute the uncertainty of the propagation speed (estimated to be 8.4–34.2%). A photodiode (Hamamatsu S6468-10) was installed at the closed end to detect the onset time of the detonation waves. The DDT run-up distance X_{ddt} and its uncertainty were estimated based on this onset time of detonation and the trajectory of the pressure wave [6].

In the subsequent set of experiments, a 38 μm thick diaphragm separated the C_3H_8/O_2 and C_3H_8/air mixtures to examine transmission of an overdriven detonation wave across a mixture. A schematic of this experimental setup is shown in Fig. 1. Based on the preliminary test, the diaphragm location from the closed end L_D was set to 152.4, 203.2 and 254 mm in an attempt to vary the strength of the overdriven detonation wave. The C_3H_8/O_2 mixture compositions were nearly stoichiometric ($\phi = 0.9, 1.0, 1$) while the C_3H_8/air mixture compositions varied from $\phi = 0.6$ –1.8. The uncertainty of the equivalence ratio of C_3H_8/O_2 mixture and C_3H_8/air mixture were ± 0.05 and ± 0.03 for 95% confidence, respectively. Two circulation pumps, one for each section, were used for about 10 minutes. Ten piezoelectric pressure transducers (PCB 113A22) were mounted along the streamwise direction. To examine the success or failure in propagating a detonation wave, a pressure transducer was mounted next to the open end at $X = 1137.9$ mm.

3 Transmission of Overdriven Detonation

3.1 Transmitted detonation wave

An idealized wave intersection model was used to calculate the states of the transmitted detonation wave D_t . With the pressure and particle velocity remaining continuous across the contact surface, the state of D_t was determined. First, the rarefaction is neglected. The intersection I_1 of the two curves DH and IE is the state of D_t , Fig. 2. Here E represents the burned products just behind the incident overdriven detonation wave. However, for the overdriven detonation wave, because the velocity of the detonation wave front relative to the burned products is subsonic, a rarefaction will follow and overtake the detonation front and further decreases the particle velocity of the burned products. Thus, the effect of the rarefaction should be considered. From the characteristic relations,

the Riemann invariant is conserved along a backward characteristic at each instant of the overdriven detonation state. Thus, the particle velocity of the burned products u_r just behind the incident overdriven detonation wave D_i is

$$u_r/c_u = [2/(\gamma + 1)](U_i/c_u) - 2/(\gamma + 1) \quad (1)$$

Here, U_i is velocity of D_i , and c_u is the sound speed in uniform region. The pressure just behind the incident overdriven detonation wave can be derived from the isentropic relations. As a result, the state of the burned products just behind the incident overdriven detonation wave changes from E to E' . Assume that E' is the state of the burned products at the moment of wave impact at the mixture interface. The state across the contact surface I_2 can be calculated by intersecting DH and IER . Table 1 shows the calculation for an incident overdriven detonation wave with degree of overdrive $D_i^* = 1.0, 1.1, 1.2, 1.3$. The table shows that the stronger incident overdriven detonation wave, the stronger is the transmitted detonation.

Table 1. Calculation results of the transmitted wave state, donor: stoichiometric C_3H_8/O_2 at 1 atm and 298 K; acceptor: stoichiometric C_3H_8/air at 1 atm and 298 K

D_i^*	$U_t(I_1)$ (m/s)	$D_t^*(I_1)$	$U_t(I_2)$ (m/s)	$D_t^*(I_2)$	$U_t(I_3)$ (m/s)	$S_t^*(I_3)$
1.0	1996	1.11	1996	1.11	1669	0.93
1.1	2493	1.39	2114	1.17	1839	1.02
1.2	2813	1.56	2268	1.26	2043	1.14
1.3	3105	1.73	2429	1.35	2242	1.25

3.2 Transmitted shock wave

Previous studies show that the transmitted detonation wave is not initiated instantaneously [7]. Thus, the transmission of the incident detonation wave can be reasonably thought to be equivalent to the transmission of a shock wave. A similar calculation as in section 3.1 was made for the transmitted shock wave S_t in which the effect of the rarefaction was also included. The results are also shown in Table 1. The velocity $U_t(I_3)$ of S_t is lower than the velocity $U_t(I_2)$ of D_t . In addition, a steady, one-dimensional, shock heating, explosion model [8] was used to calculate the induction time after the shock heating of reactive gas mixtures. The calculations show the Mach number and postshock temperature increase while τ decreases with a higher D_i^* . To instantaneously initiate a transmitted detonation wave, a high D_i^* is required.

4 Results and Discussion

The results of the preliminary test on the effect of the degree of overdrive D^* on the DDT run-up distance for different tube diameters are shown in Fig. 3 (left). The decay of D^* is correlated with X/X_{ddt} . We can see that D^* decreases with increasing X/X_{ddt} . The length of decay of the overdriven detonation wave as it approaches the CJ detonation is estimated to be about $2X/X_{ddt}$. From these observations, we can conclude that in order to obtain a high D^* for the incident overdriven detonation wave, the interface of mixture change should be placed close to the DDT location.

The experimental results of the wave transmission process reveal that the wave transmission can be classified into three modes:

- A. Decay from an overdriven state to a lower overdrive, and decay to a near-CJ state.
- B. Decay from an overdriven state to a lower overdrive, and accelerate to a higher overdrive, and then decay to a near-CJ state.
- C. Decay from an overdriven state to a sub-CJ state, and transition to an overdriven state, and then decay to a near-CJ state.

Examples of these three modes of wave transmission are shown in Fig. 3 (right). For mode A, two distinct modes are observed. The displacement-time diagram for mode A1 is shown in Fig. 4 (left). The highly overdriven detonation wave decays abruptly at the diaphragm and then maintains an overdriven state ($D_t^* = 1.43$). This overdriven detonation wave gradually decays to a near-CJ state ($D_t^* = 0.9$). In this mode, a transmitted overdriven detonation wave was obtained because of the high D_i^* . The rarefaction led to the continuous decay of the transmitted overdriven detonation wave. Because the cell width λ depends on the degree of overdrive, the decay process will increase λ . Once λ becomes so large that it lies outside the detonability limit $d > \lambda$, the detonation wave fails to be sustained. For $\phi_t = 0.94$, $\lambda \approx 60$ mm at the CJ detonation state, which is larger than the tube diameter. This is the most likely interpretation that a detonation wave is not found.

Figure 4 (right) shows the displacement-time diagram for mode A2. The transmitted overdriven detonation wave after diaphragm rupture was obtained with $D_t^* = 1.32$ and gradually decayed to a near-CJ state. Then an overdriven detonation wave with $D_t^* = 1.17$ was found after the attenuation process. Further downstream the attenuation process occurred again. This repeated process of decay, transition, and decay was regarded as an unstable detonation wave [9].

In mode B, the slightly overdriven state of $D_t^* = 1.07$ is obtained after the diaphragm rupture. However, a gradual acceleration took place to develop a higher degree of overdrive at $D_t^* = 1.25$. Then the overdriven detonation wave decayed to a near-CJ state of $D_t^* = 0.93$ just as for modes A1 and A2. For the acceleration process to occur instead of an attenuation process after diaphragm rupture, it is thought that a transmitted shock wave was formed. Because of the less reactive mixture in this case ($\phi_t = 0.76$), the induction time to react was too long and the detonation wave was not able to be initiated instantaneously, as discussed in section 3.2. In mode C, a sub-CJ state where $D_t^* = 0.77$ was observed after the diaphragm rupture. The strength of the incident overdriven detonation wave of this mode ($D_i^* = 1.08$) is apparently lower than the other modes. Thus, a transmitted shock wave is formed. Then the transition to an overdriven detonation wave takes place.

Among these modes, an unstable detonation wave appears in modes A2 and C, which was found in most of the tests. Mooradian and Gordon [9] noted the unstable detonation wave near the detonability limit as the overdriven detonation wave decays approaching the CJ state. Otherwise, it can be noticed that there is no detonation wave near the open end in some modes, Fig. 5. The figure shows that the survival of the detonation wave is mainly related to the mixture composition and the detonation wave propagating velocity. The critical conditions are $\phi_t \geq 0.87$ and $D_t^* \geq 0.82$, which are directly connected to λ . This implies that the detonability limit is the dominant factor in the propagation of the detonation wave after the process of wave transmission.

5 Conclusions

In wave transmission process, a transmitted overdriven detonation wave takes place instantaneously when a strong incident overdriven detonation wave is used. A near-CJ state of the incident wave leads to a transmitted shock wave, and then the transition to an overdriven detonation occurs downstream. Whenever the transmitted overdriven detonation wave is attained instantaneously or by transition, the process of the transmitted overdriven detonation wave decaying to a near-CJ state occurs in all tests. In most tests, there is an unstable detonation wave observed after the attenuation process approaching to a near-CJ state. This may be attributed to that the increase of the cell width in the attenuation process lies outside the detonability limits.

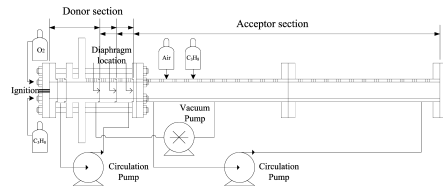


Fig. 1. Experimental facility and instrumentation

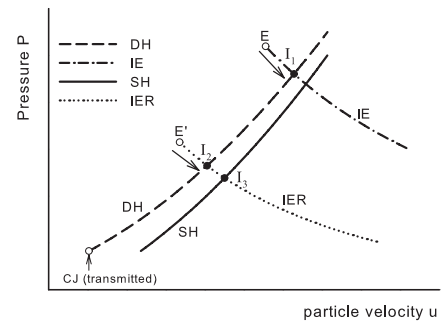


Fig. 2. $P-u$ diagram; IE : isentropic-expansion curve passing D_i product; IER : IE curve considering rarefaction; DH : the locus of all possible final states for the D_t ; SH : the locus of all possible postshock states

References

1. J.O. Sinibaldi, C.M. Brophy, C. Li, K. Kailasanath: AIAA paper 2001-3466 (2001)
2. E. Schultz, J.E. Shepherd: *Detonation Diffraction through a Mixture Gradient*, Technical Report FM00-1, GALCIT (2000)
3. D. Desbordes, A. Lannoy: Effects of a Negative Step of Fuel Concentration on Critical Diameter of Diffraction of a Detonation. In: *Dynamics of Detonations and Explosions: Detonations*, Progress in Astronautics and Aeronautics, vol 133, ed by A.L. Kuhl et al. (AIAA, 1991) pp 170-186
4. P.A. Urtiew, A.K. Oppenheim: *Proc. R. Soc. Lond. A* **295** (1966) 13-28
5. R. Knystautas, J.H. Lee, O. Peraldi, C.K. Chan: Transmission of a Flame from a Rough to a Smooth-Walled Tube. In: *Dynamics of Explosions*, Progress in Astronautics and Aeronautics, vol 106, ed by J.R. Brown et al. (AIAA, 1986) pp 37-52
6. J. Li, W.H. Lai, K. Chung, F.K. Lu: *Shock Waves* **14** (5-6) (2005) 413-420
7. M.S. Kuznetsov, V.I. Alekseev, S.B. Dorofeev, I.D. Matsukov, J.L. Boccio: *Proc. Combust. Inst.* **27** (1998) 2241-2247
8. R.E. Mitchell, R.J. Kee, SHOCK: A General Purpose Computer Code for Predicting Chemical Kinetic Behavior behind Incident and Reflected Shocks, SAND82-8205 (1982)
9. A.J. Mooradian, W.E. Gordon: *J. Chem. Phys.* **19** (9) (1951) 1166-1172

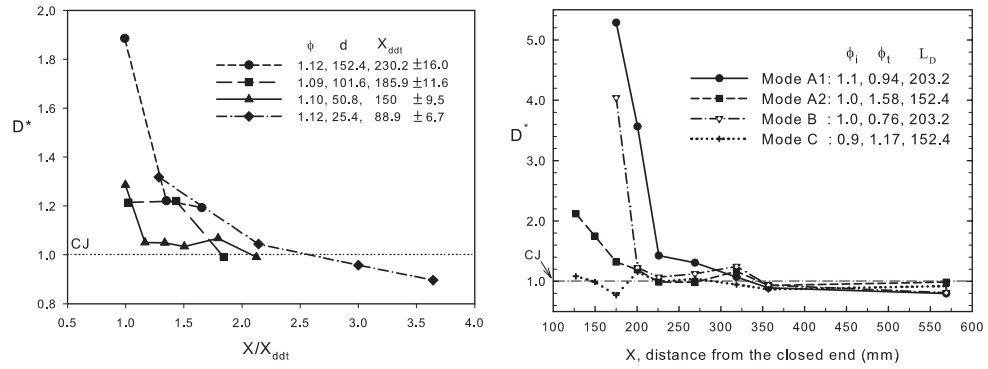


Fig. 3. Degree of overdrive with different tube diameters (left); modes of wave transmission process (right)

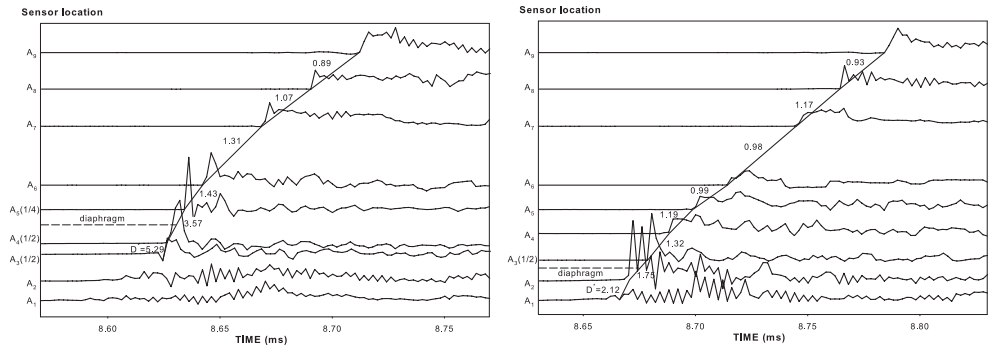


Fig. 4. The displacement-time diagram for mode A1 (left); the displacement-time diagram for mode A2 (right)

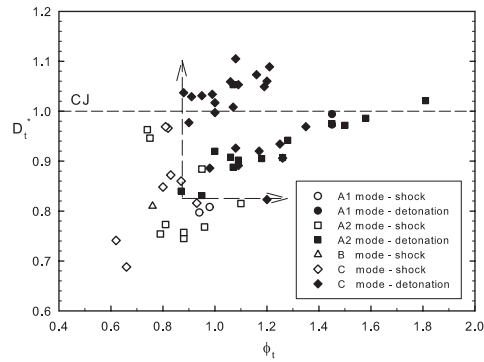


Fig. 5. The wave behavior near the open end for all tests